Improved alternating gradient transport and focusing of neutral molecules

Juris Kalnins, Glen Lambertson, and Harvey Gould[a)]
Mail Stop 71-259, Lawrence Berkeley National Laboratory, University of California, Berkeley, California 94720

(Received 27 December 2001; accepted for publication 12 February 2002)

Polar molecules, in strong-field seeking states, can be transported and focused by an alternating sequence of electric field gradients that focus in one transverse direction while defocusing in the other. We show, by calculation and numerical simulation, how one may greatly improve the alternating gradient transport and focusing of molecules. We use a new optimized multipole lens design, a FODO-lattice beam transport line, and lenses to match the beam transport line to the beam source and to the final focus. We derive analytic expressions for the potentials, fields, and gradients that may be used to design these lenses. We describe a simple lens optimization procedure and derive the equations of motion for tracking molecules through a beam transport line. As an example, we model a straight beamline that transports a 560 m/s jet-source beam of methyl fluoride 15 m from its source and focuses it to 2 mm diameter. We calculate the beam transport line acceptance and beam survival, for a beam with a velocity spread, and estimate the transmitted intensity for specified source conditions. Possible applications are discussed.
[DOI: 10.1063/1.1485778]

I. INTRODUCTION

A polar molecule has an intrinsic separation of charge on which an electric field gradient exerts a force. The force F_x in the (transverse) x direction is

$$F_x = -\frac{\partial W}{\partial x} = -\frac{\partial W}{\partial E}\frac{\partial E}{\partial x}, \tag{1}$$

where W is the potential energy of the molecule in an electric field E (Stark effect) of magnitude $E=(E_x^2+E_y^2)^{1/2}$; and similarly for the force, F_y in the y direction. The force and gradient are in opposite directions (weak-field seeking) for rotational states that become less tightly bound in an electric field ($\partial W/\partial E > 0$), while the force and gradient are in the same direction (strong-field seeking) for rotational states that become more tightly bound in an electric field ($\partial W/\partial E < 0$). The $J=0$ state is always strong-field seeking and all rotational states become strong-field seeking in the limit of strong electric field as shown in Fig. 1.

Focusing a beam of molecules, traveling in the z direction, is achieved using static two-dimensional (x,y) electric field gradients. We neglect end field effects and assume $E_z = 0$ inside the focusing lenses. Molecules in weak-field seeking states can be focused, in both directions, using quadrupole and/or sextupole fields that have a minimum in the electric field in both directions. Molecules in strong-field seeking states, however, can be focused in only one transverse direction, while being defocused in the other, because it is not possible to have a maximum in the electric field in both dimensions (in free space).

Molecules in strong-field seeking states have been transported and focused by an alternating sequence of electric field gradient lenses[1–7] (as have neutral atoms[8]), but it has been neither as successful, nor as widely used, as has quadrupole and sextupole focusing for molecules in weak-field seeking states.[7,9]

In this article we show, by calculation and numerical simulation, how one may greatly improve the alternating gradient transport and focusing of molecules by optimizing the lens field geometries so that nonlinearity in $\partial W/\partial E$ is compensated by $\partial E/\partial x$ to produce a linear restoring force. We use this optimized multipole lens design in a FODO-lattice beam transport line and use additional lenses to match the beam transport line to the beam source and to the final focus.

The remainder of this article is organized as follows: Sec. II discusses alternating gradient focusing, transport lattices, matching lenses, and linear optics. Section III derives the formulas for designing linear focusing elements and presents examples of lenses. Section IV derives the equations for molecular beam transport and models both a simple 30-m-long FODO lattice and a complete 15-m-long transport line with entrance and exit matching lenses. Section IV G estimates the intensity of a methyl fluoride jet-source beam, transported through a beamline and focused. Section V discusses the use of strong-field seeking states, and possible applications of alternating grading focusing and transport through very long beamlines.

II. ALTERNATING GRADIENT BEAM TRANSPORT AND FOCUSING

A beam of charged particles can be focused and transported over almost unlimited distances by alternating F and D-type magnetic quadrupole lenses. The F-type lens focuses the beam in the horizontal (x) direction while defocusing it in

[a)]Author to whom correspondence should be addressed; electronic mail: gould@lbl.gov

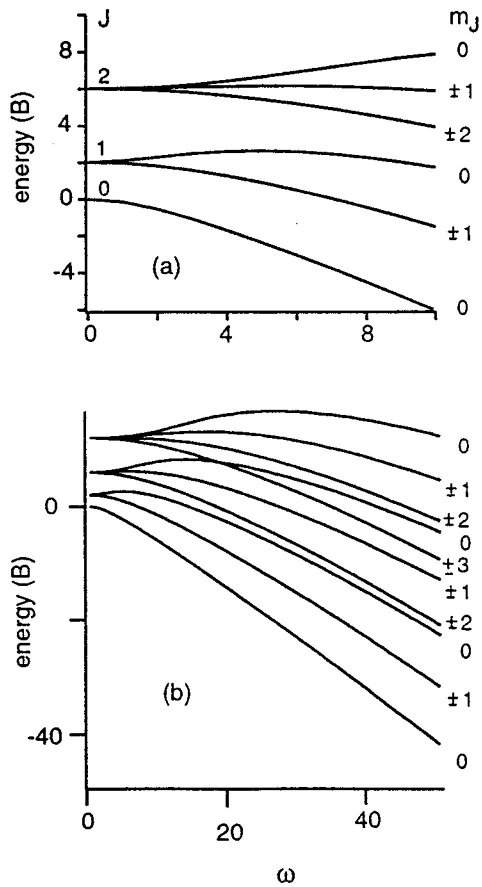

FIG. 1. Energy levels of low-lying rotational states of a diatomic or symmetric-top molecule in an electric field (Stark effect). The levels were calculated using the rigid rotor model. The horizontal axis is in dimensionless units of $\omega = d_e E/B$, where d_e is the electric dipole moment, E the electric field, and B the rotational constant. The vertical axis is in units of B. Energies for small ω are shown in (a) and energies for large ω in (b). The potential energy of the molecule, W, is the change in energy from zero electric field and for very large ω, $W \rightarrow d_e E$. The levels that descend are strong-field seeking. For the $J=0$ state of methyl fluoride (CH_3F), in the $K=0$ state, $\omega=1$ at 2.78 MV/m. For the $J=0$ state of CsF, $\omega=1$ at 0.135 MV/m.

the vertical (y) direction. The D-type defocuses the beam in the horizontal direction while focusing it in the vertical direction.

A complete alternating gradient transport line begins with a beam source whose output is optically matched, by lenses, into the acceptance of a transport section which in turn is matched, by lenses, to a final focus. The final focus can be, for example, at an experimental target or at a matching point for injection into a (storage) ring lattice. A complete transport line for molecules, starting with a jet source and skimmer, is shown in Fig. 2. For long-distance beam transport, the lens system providing the highest beam acceptance and requiring the lowest focusing strength is a lattice of identical FODO cells, in which the F/D lenses are separated by drift spaces (O).

To match the molecular beam source to the transport line, and to match the transport line to the final focus, we use doublet (FD/DF) and triplet (FDF/DFD)-type lens configurations. These lens configurations generally require higher focusing strengths than do the FODO cells. Doublets are typically used for asymmetric focal points (unequal x and y dimensions) while triplets are used for symmetric ones. In the F/D doublet, a net focusing in x and y occurs because particles first focused in x are, in the second element, closer to the axis and therefore less defocused. Particles first defocused in y are, in the second element, further from the axis and thus more strongly focused.

In all lenses, linear focusing is needed for optimum optical properties. Linear focusing requires that the force in each direction by linearly proportional to the displacement in that direction ($|F_x/x| = \text{constant}$ and $|F_y/y| = \text{constant}$), and independent of the displacement in the other direction (uncoupled motion). Strong nonlinearities in focusing elements will result in loss of beam, generation of beam halo, and growth in the transverse emittance (the product of the angular divergence and the spatial dimension) producing larger beam sizes.

III. LINEAR OPTICS

A. Potential energy of a molecule in an electric field

To determine the lens shape that will produce the most linear force on the molecule, we need $\partial W/\partial E$ for Eq. (1). This quantity will change with the $J,|m_J|$ rotational state and the electric field strength. If a number of rotational levels have a similar $\partial W/\partial E$, then one lens design will be nearly optimum for all of them. In the limiting case of a strong electric field, $\partial W/\partial E = -d_e$, where d_e is the electric dipole moment. This is shown in Fig. 1 for large $\omega = d_e E/B$, where B is the rotational constant.

For polar molecules in weaker fields, we calculate the interaction energy, in the rigid rotor approximation, following the approach of von Meyenn.[10] The Hamiltonian operator is $H = B\mathbf{J}^2 - d_e E \cos\theta$, where B is the rotational constant, and the direction cosine matrix elements, which couple (J,m_J) with $(J+1,m_J)$ and $(J-1,m_J)$, are taken from Townes and Schawlow.[11] We diagonalize the matrix for terms through $J=30$. The first few levels are shown in Fig. 1.

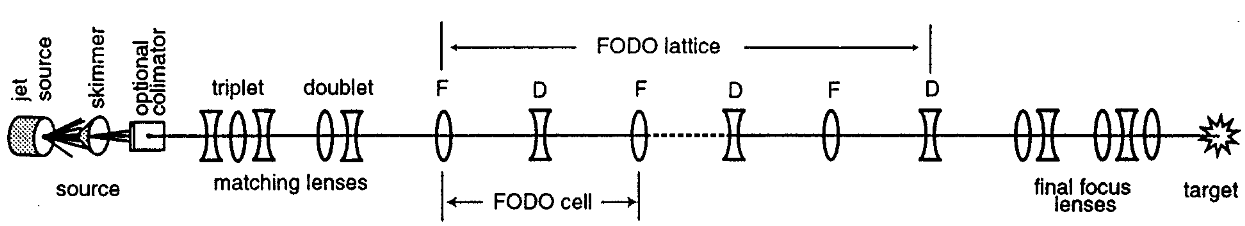

FIG. 2. Schematic diagram of an alternating gradient beam transport line for molecules. It consists of a jet source and skimmer, beam matching optics, FODO lattice, and final focus optics.

As $\omega = d_e E/B$ and B determine the Stark effect for each $J,|m_J|$, it is straightforward to construct a simple function for the Stark effect for any $J,|m_J|$. For the $J=0$ state of a diatomic molecule or symmetric top ($K=0$) molecule, a satisfactory approximation[12] is

$$W(E) = \frac{C_1 \omega^2 B}{1 + C_2 \omega} = \frac{C_1 d_e^2 E^2}{B + C_2 d_e E} \tag{2}$$

with $C_1 = -0.2085$ and $C_2 = 0.2445$. This expression works best for small and intermediate values of ω.

From Eq. (2), for the $J=0$ state, the field derivative of the potential is

$$\frac{\partial W}{\partial E} = \frac{W}{E}\left[\frac{2B + C_2 d_e E}{B + C_2 d_e E}\right]. \tag{3}$$

Similar expressions may be found for other rotational levels. A perturbation expression for W can be used for rotational states in (very) weak electric fields.[11] In some applications, using $\partial W/\partial E$ from either the strong-field limit or the weak-field limit will be sufficient to design a linear lens.

Finally, we note that all atoms and molecules, including nonpolar molecules, are polarizable with an interaction energy $W_\alpha = -\frac{1}{2}\alpha E^2$, where α is the dipole polarizability.[13,14] For laboratory electric fields this interaction is much smaller than the interaction with a molecular electric dipole moment, but it can be used to focus atoms[8] or decelerate them.[15]

B. Electric field gradient of a focusing lens

Any lens potential, Φ can be expressed as the following multipole expansion in cylindrical coordinates, r, θ:

$$-\Phi(r,\theta) = E_0 r_0 \left[\sum_{n=1}^{\infty} \frac{b_n}{n}\left(\frac{r}{r_0}\right)^n \cos(n\theta) + \sum_{n=1}^{\infty} \frac{a_n}{n}\left(\frac{r}{r_0}\right)^n \sin(n\theta)\right],$$

where E_0 is the central field $[E = E_0(b_1^2 + a_1^2)^{1/2}]$, r_0 is a scaling length, and $b_n(a_n)$ are the dimensionless constants of the $2n$-pole strengths for normal (skew) elements.

Setting $b_n = a_n$ for simplicity, converting to Cartesian coordinates, and retaining only the a_1, a_3, and a_5 terms (see Sec. III C), the lens potentials for normal multipoles are

$$-\Phi_N(x,y) = E_0 x\left[a_1 + \frac{a_3(x^2 - 3y^2)}{3r_0^2} + \frac{a_5(x^4 - 10x^2y^2 + 5y^4)}{5r_0^4}\right] \tag{4}$$

or for skew multipoles are

$$-\Phi_S(x,y) = E_0 y\left[a_1 + \frac{a_3(3x^2 - y^2)}{3r_0^2} + \frac{a_5(5x^4 - 10x^2y^2 + y^4)}{5r_0^4}\right], \tag{5}$$

where E_0 is the field on axis for $a_1 = 1$.

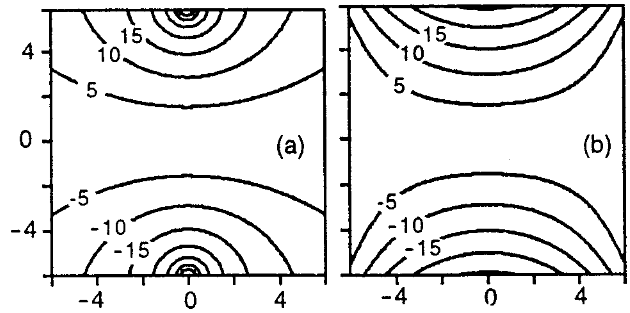

FIG. 3. Equipotentials (truncated) in x and y of skew F lenses. The actual electrode can be fabricated from any set of equipotentials and, if dimensions are in mm, they match lenses used in the examples in Sec. IV. A two-wire field lens (with multipole components: $a_1 = 1$, $a_3 = -1$, $a_5 = 1$,...) is shown in (a). An optimized multipole lens (with multipole strengths $a_1 = 1$, $a_3 = -3$, $a_5 = 0$) is shown in (b). The lens in (b) is designed to focus in the strong-field limit.

Both of these potentials give the same total electric field ($E = -\nabla\Phi$)

$$E(x,y) = (E_x^2 + E_y^2)^{1/2} = E_0\left[a_1^2 + \frac{2a_1a_3(x^2 - y^2)}{r_0^2} + \frac{a_3^2(x^4 + 2x^2y^2 + y^4)}{r_0^4} + \frac{2a_1a_5(x^4 - 6x^2y^2 + y^4)}{r_0^4} + \cdots\right]^{1/2} \tag{6}$$

which has the electric field gradients

$$\frac{\partial E}{\partial x} = \frac{2a_3E_0^2}{r_0^2}\frac{G_x x}{E}, \qquad \frac{\partial E}{\partial y} = -\frac{2a_3E_0^2}{r_0^2}\frac{G_y y}{E}, \tag{7}$$

where

$$G_x(x,y) = a_1 + \frac{a_3(x^2 + y^2)}{r_0^2} + \frac{2a_1a_5(x^2 - 3y^2)}{a_3 r_0^2} + \cdots,$$
$$G_y(x,y) = a_1 - \frac{a_3(x^2 + y^2)}{r_0^2} + \frac{2a_1a_5(3x^2 - y^2)}{a_3 r_0^2} + \cdots. \tag{8}$$

C. Force on the molecule due to an electric field gradient

The force on a polar molecule in the x or y direction can now be calculated using Eqs. (1), (7), and (8) with a suitable expression for $\partial W/\partial E$ from Sec. III A.

Nonlinear forces, inside the focusing lenses, limit the maximum beam size that one can transport without suffering beam losses, emittance (size) growth, and beam halo. Nonlinear forces generally arise from higher-order multipole components of the lens electrostatic potential. Cylindrical electrodes, which are two-wire field lenses (with r_0 = half gap), shown in Fig. 3(a), have long been used to focus molecules in strong-field seeking states.[1–7] They contain multipoles of all odd orders and of equal strengths ($a_1=1$, $a_3=-1$, $a_5=1$,...). As we will see below, its strong decapole field ($a_5=1$) reduces the area of the lens over which the focusing is linear (dynamic aperture). A beam transport line using two-wire field lenses will be limited to a smaller diameter beam compared to a similar transport line using an optimized multipole lens such as the one shown in Fig. 3(b).

To produce a larger linear region we try to limit the multipole fields to those that are essential for the optics. We include a dipole field (a_1) to give a nonzero field on axis, without which strong-field seeking molecules defocus in both transverse directions; a sextupole field (a_3) to provide the linear focusing force (of order r^1); and a decapole field (a_5) to correct the nonlinear forces (of order r^3) produced by the sextupole field. We omit the quadrupole field (a_2), because it bends the beam, and we omit the octupole field (a_4), because it introduces stronger nonlinear forces (of order r^2) than those of the sextupole/decapole fields. All other multipole strengths are set to zero. In a real lens, however, the electrodes may be truncated equipotentials, with the consequence that small residual higher order multipoles will remain.

Since the lens potentials, as defined by Eqs. (4) and (5), have two free parameters, we chose $a_1=1$, making E_0 the central field and we choose $|a_3|=1$, making it easier to compare the optimized multipole lens to a two-wire field lens. The remaining choice is the decapole field strength a_5, which we use to optimize the lens optics. We do this in two ways: first by calculating, for specific molecules, the forces F_x and F_y inside a lens and comparing their linearity in x and y for different a_5, and second, in Sec. IV, by simulation of beams in model transport lines.

If we calculate the horizontal force, F_x on a molecule whose potential energy is $W=-d_eE$ (strong-field limit), we find that it is most linear on axis ($y=0$) for no decapole field ($a_5=0$). For this example, the constant-force contours for F_x in the x,y plane are shown, for the two-wire field lens, in Fig. 4(a) and, for the zero-decapole lens, in Fig. 4(b). The zero-decapole lens is seen to have far better linearity than the two-wire field lens. (This is also true for F_y which is not shown here.) In a similar way, we find that the optimized multipole lens outperforms the two-wire field lens in the low electric field limit (quadratic Stark effect), where the most linear field on axis has $a_5=-\frac{1}{2}$.

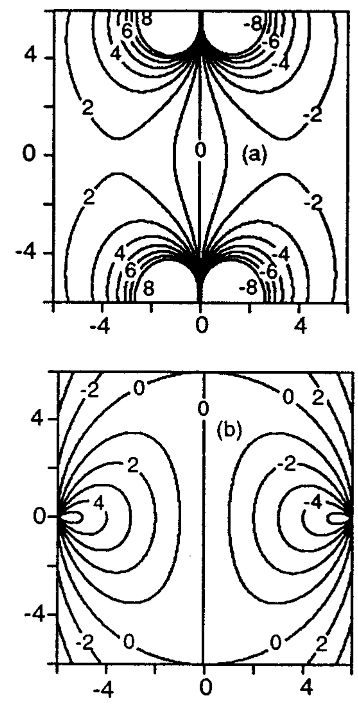

FIG. 4. Contour plots of the force in the x direction (F_x), on a molecule inside a lens, as a function of x and y position. The lines are contours of equal F_x in arbitrary units. In this example we use the large Stark effect limit ($W=-d_eE$) and $r_0=6$ mm. (a) F_x for a two-wire field lens. (b) F_x for an optimized multipole lens ($a_5=0$). A lens that was completely linear in F_x would have vertical contour lines with uniform spacing.

D. End effects

Real lenses have finite length, and the two-dimensional fields inside become three-dimensional fields at the ends. There are three effects from this. First, the z component of the field gradient affects the transverse motion. This will be small if the lens aperture is small compared to the physical length of the lens.

Second, the lens field acts over a distance that is different than the physical length of the electrodes because of (extending) fringe fields at the ends. For linear design optics we approximate the real lens by a lens of constant central field E_0 over an effective length, different that the physical length of the lens. The effective length is determined by integrating the actual central field (found by numerical calculation or measurement) through the lens, including the ends, and dividing by E_0.

Third, the z component of the electric field gradient, present at the ends of the lens, has an effect on the z-component (longitudinal) velocity. The nonrelativistic Hamiltonian (neglecting gravity) for a molecule of mass m and total velocity v is: $H=\frac{1}{2}mv^2+W$. The Hamiltonian is conserved if the electric field is static. Consequently, a molecule in a strong-field seeking (weak-field seeking) state will gain (lose) kinetic energy entering the lens and then lose (gain) the same amount of kinetic energy upon exit.[15,16] For the central ($x=y=0$) trajectory, the longitudinal velocity, v_{zE}, of the molecule, in the lens is

$$v_{zE}^2=v_{z0}^2-W/2m,$$

where v_{z0} is the velocity of the molecule in the drift spaces. For most thermal or jet-source molecules in laboratory electric fields, the change in velocity is a small effect. (A beam of 560 m/s methyl fluoride molecules in the $J=0$ state increases its velocity by 0.2 m/s upon entering an electric field of 10 MV/m.)

IV. BEAM TRANSPORT

A. Equations of motion

To track the trajectories of molecules passing through combinations of lenses, we use the transverse nonlinear equations of motion for a molecule traveling in the z direction, given from Eqs. (1), (7), and (8):

$$x'' + \frac{2a_3}{r_0^2}\frac{E_0^2}{mv_{ZE}^2}\frac{G_x x}{E}\frac{\partial W}{\partial E} = 0,$$
$$y'' - \frac{2a_3}{r_0^2}\frac{E_0^2}{mv_{ZE}^2}\frac{G_y y}{E}\frac{\partial W}{\partial E} = 0 \quad (9)$$

with trajectory gradients defined as $x' = dx/dz = v_x/v_{ZE}$ and $y' = dy/dz = v_y/v_{ZE}$.

We start the design optics using completely linear lenses ($G_x = G_y = 1$, and $E = E_0$), for which Eq. (9) reduces to

$$x'' + K_0 x = 0 \quad y'' - K_0 y = 0, \quad (10)$$

where K_0 is the lens linear focusing strength

$$\begin{aligned} K_0 &= \frac{2a_3}{r_0^2}\frac{E_0}{mv_{ZE}^2}\frac{\partial W}{\partial E} \\ &= -\frac{2a_3}{r_0^2}\frac{d_e E_0}{mv_{ZE}^2} \quad \text{for } W = -d_e E \\ &= -\frac{2a_3}{r_0^2}\frac{\alpha E_0^2}{mv_{ZE}^2} \quad \text{for } W_\alpha = -\frac{1}{2}\alpha E^2 \\ &= \frac{2a_3}{r_0^2}\frac{d_e^2 E_0^2}{mv_{ZE}^2}\frac{C_1(2B + C_2 d_e E_0)}{(B + C_2 d_e E_0)^2} \\ &\quad \text{for } J = 0, \text{ from Eq. (2).} \end{aligned} \quad (11)$$

For a molecule in a strong-field seeking state ($\partial W/\partial E < 0$), the lens will focus in the x direction (F lens) for $a_3 < 0$, and focus in the y direction (D lens) for $a_3 > 0$. For a molecule in a weak-field seeking state ($\partial W/\partial E > 0$) the F and D directions are reversed. The lenses can also be used to focus atoms ($\partial W_\alpha/\partial E = -\alpha E$) which, in their ground states, are always strong-field seeking.

The linear design optics will determine the lens focusing strength K_0. Then, the choice of scaling radius, r_0, will give the required lens field, E_0, from Eq. (11). Small r_0 allows us to use low electric fields but, as seen from Eqs. (6) and (8), large r_0 is needed for increased linearity. The value of r_0 chosen will then depend on the maximum electric field strength and the beam size to be transported.

B. Example of methyl fluoride

For a realistic beam transport simulation, we assume a beam of methyl fluoride (CH_3F), in the $J = 0$ rotational state, having a longitudinal velocity $v_{Z0} = 560$ m/s. This is the approximate velocity of a beam produced by seeding methyl fluoride in an argon jet source with a reservoir temperature of 300 K (see Sec. IV G). The electric field derivative of the potential energy (of the $J = 0$ state), is given by Eq. (3) with $d_e = 6.25 \times 10^{-30}$ J/V/m (1.86 Debye) and rotational constant $B = 1.76 \times 10^{-23}$ J (0.88 cm^{-1}).

To study long distance transport, we model a FODO lattice consisting of a sequence of identical F and D lenses separated by drift spaces (O). Then, to study a complete beamline, we add an upstream lens section, to match the beam from the jet source into the FODO lattice, and a downstream section for a final focus on the beam (see Fig. 2).

C. FODO lattice

We chose a simple FODO lattice consisting of identical FODO cells (see Sec. II). The optics of a FODO cell starts in the center of an F lens (or D lens) and ends at the center of the next F lens (or D lens). At the ends of the FODO cell the beam is at a waist (defined as zero slope in the beam size) with a maximum size in one plane and a minimum size in the other plane.

For this study, we use 10-cm-long F/D lenses, with scaling length $r_0 = 6$ mm, separated by 40 cm drift spaces, giving a FODO cell length of 100 cm. This design leaves 80% of the cell unfilled. It is economical to build, but does not have as large an acceptance as designs that filled more of the lattice (see Sec. V).

In a FODO lattice the motion of a particle is periodic in phase space. The phase advance measures how far along the period it has proceeded from its initial starting point. The transverse linear optics are characterized by the phase advance in the FODO cell μ_c. For our cell we choose $\mu_c = \pi/3$ rad, for which all particles return to their initial phase-space position after 6 FODO cells. This specifies a central field of $E_0 = 3.23$ MV/m, which is not close to breakdown, as well as a beam size that is nearly the minimum possible.

D. Modeling beam transmission

1. Beam distribution in phase space

We take the molecular beam to be continuous (unbunched) and monoenergetic, in which case, it is completely specified by its density in the (x, x', y, y') phase space (distribution function). The beam size in a transport line depends, not on the density, but on the four-dimensional volume V_{4D} occupied by the beam. This can be defined, experimentally, in a number of ways: (a) the volume containing some fraction of the beam, (b) the volume calculated from the root-mean-square (rms) beam sizes, or (c) the volume defined by a set of collimators. These four-dimensional volumes can be related to an equivalent theoretical distribution function of Kapchinsky and Vladiminsky (KV).[17] With the KV distribution function, we can calculate the linear focusing beam sizes (a_x, a_y) along the beam transport line and, in so doing, model the design optics.

The KV distribution consists of a uniform density of particles on a hyper ellipsoid in four-dimensional phase space. At a beam waist ($a_x' = a_y' = 0$), the hyper ellipsoid is given by

$$\left(\frac{x}{a_x}\right)^2 + \left(\frac{x'}{a_{x'}}\right)^2 + \left(\frac{y}{a_y}\right)^2 + \left(\frac{y'}{a_{y'}}\right)^2 = 1 \quad (12)$$

and has the volume, $V_{KV} = \frac{1}{2}\pi^2 a_x a_{x'} a_y a_{y'}$. Typically we have beam waists at the beam source (minimum), at any focus (minimum), and inside the focusing lenses (minimum or maximum).

The beam sizes along the beam transport line are given by the uncoupled envelope equations, which for the equations of motion [Eq. (10)] are

$$a_x'' + K_0 a_x = \frac{\epsilon_{\mathrm{KV}x}^2}{a_x^3},$$
$$a_y'' - K_0 a_y = \frac{\epsilon_{\mathrm{KV}y}^2}{a_y^3}, \tag{13}$$

where $\epsilon_{\mathrm{KV}x}$ and $\epsilon_{\mathrm{KV}y}$ are the invariant transverse emittances which, at a waist [see Eq. (12)], are simply given by $\epsilon_{\mathrm{KV}x} = a_x a_{x'}$ and $\epsilon_{\mathrm{KV}y} = a_y a_{y'}$.

If we project the KV distribution onto the (x,x') plane, we obtain a uniform density of particles inside an ellipse of constant area $\pi\epsilon_{Kvx}$. For an arbitrary beam distribution, the equations of motion, for the rms beam sizes, have the same form as Eq. (13). This defines the rms-equivalent KV distribution sizes as $a_x = 2\sigma_x, a_{x'} = 2\sigma_{x'}, a_y = 2\sigma_y$, and $a_{y'} = 2\sigma_{y'}$. Under linear forces, a molecule remains on the same KV surface on which it started, with the shape of the ellipse changing but its volume remaining constant.

Since the nonlinear forces inside a lens become stronger, the further the molecule is from the central axis, lenses may be evaluated by computing the increase in nonlinear effects with increasing beam size. For this we use nested KV distributions of increasing volume, each of which is characterized by its volume, V_{KV}. The simulation results are then independent of the characteristics of the initial beam and can be applied to nonsurface beam distributions.

2. Beam survival

We calculate the survival of a 560 m/s methyl fluoride beam in the $J=0$ state, through a 30 m FODO lattice, as a function of the decapole strength (a_5). The lattice is described in Sec. IV C, and we assume that the beam is already matched to the lattice. As molecular beam jet sources are usually axisymmetric, we take the emittance, ϵ_{KV} to be the same in both transverse planes. Then, the initial matched beam sizes and divergences, for the $\pi/3$ phase-advance FODO cell, are

$$a_{\max} = a_x = (\epsilon_{\mathrm{KV}}\beta_{\max})^{1/2},$$
$$a_{x'} = (\epsilon_{\mathrm{KV}}\beta_{\max})^{1/2},$$
$$a_y = (\epsilon_{\mathrm{KV}}\beta_{\min})^{1/2},$$
$$a_{y'} = (\epsilon_{\mathrm{KV}}\beta_{\min})^{1/2},$$

where $\beta_{\min}=0.587$ m and $\beta_{\max}=1.703$ m. As β is independent of the emittance, we use the initial maximum beam size, $a_{\max}$, as our KV distribution size parameter

$$V_{\mathrm{KV}} = \frac{1}{2}\pi^2\epsilon_{\mathrm{KV}}^2 = \frac{\pi^2 a_{\max}^4}{2\beta_{\max}^2}.$$

The relation between the beam size and the emittance is shown in Fig. 5.

The trajectories were numerically integrated along the FODO lattice using a fourth-order Runge–Kutta algorithm. We take as lost those particles whose transverse displacement, in the beam transport line, in x and/or y became too large. The transported particles, which started on a zero-thickness KV surface, finished up on a smeared-out fuzzy one, producing emittance growth and halo.

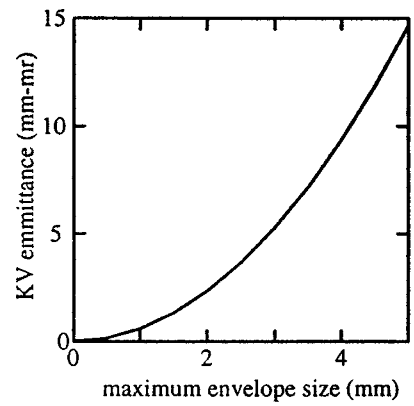

FIG. 5. Emittance vs beam envelope size of the shell in the Kapchinsky–Vladimirsky (KV) equilibrium beam distribution.

From the simulations, we found the fraction of the initial methyl fluoride beam surviving as a function of position along the beamline. We did this for two different lens designs (two-wire field lens and optimized multipole) and for selected initial KV beam sizes. The results are shown in Figs. 6(a) and 6(b).

For the two-wire field lens, the largest KV beam that can be transmitted without loss is 1.4 mm. For the optimized

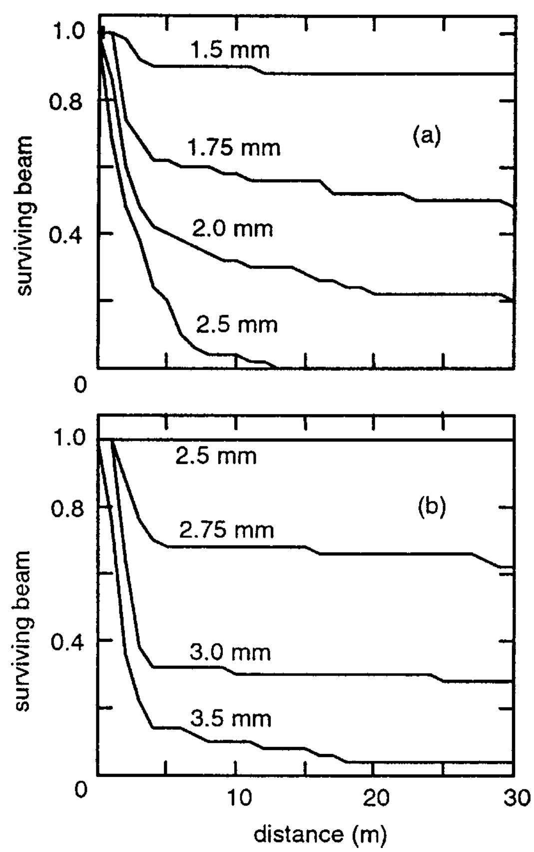

FIG. 6. Calculated beam survival for 560 m/s methyl fluoride in the $J=0$ state in a 30-m-long FODO lattice constructed of (a) two wire lenses or (b) optimized multipole lens with $a_5=0$. In each case $r_0=6$ mm and the central field, $E_0=3.2$ MV/m. Survival is plotted for various (KV) beam sizes. For the 100% beam survival, the beam intensity scales as KV beam size to the fourth power. Consequently, the FODO lattice of optimized multipole lenses will transport about a factor of 10 more beam than the same FODO lattice of two-wire field lenses.

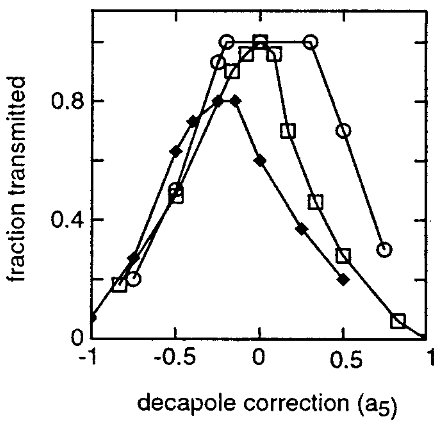

FIG. 7. Survival of 560 m/s monoenergetic beams through the 30 m FODO lattice for a KV beam with $a_{max}=2.5$ mm as a function of decapole constant (a_5). Results for a methyl fluoride at 3.2 MV/m are shown as open squares, the limiting cases of very strong and very weak electric field as open circles, and filled diamonds, respectively.

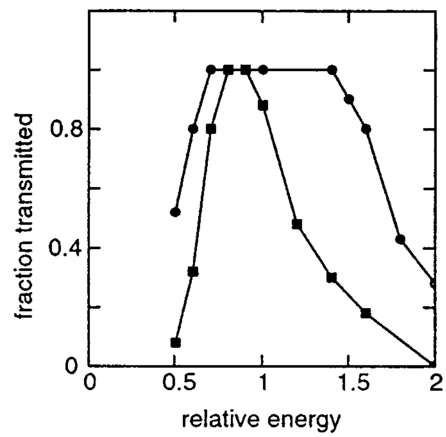

FIG. 8. Calculated transmission, as a function of relative beam kinetic energy, of a beam of methyl fluoride in the $J=0$ state through a 30 m FODO lattice. The nominal energy is 640 K (560 m/s) and the KV beam size is $a_{max}=1.5$ mm. Points for the FODO lattice using two-wire field lenses and optimized multipole lenses (with decapole constant $a_5=0$) are shown as squares and circles, respectively.

multipole lens, the largest lossless KV beam is 2.5 mm. If the initial phase-space density of the beams is approximately constant, the relative beam intensity is given by the ratio of the lossless phase-space volumes. *This is a factor of* $(2.5/1.4)^4 \approx 10$ *improvement by using the optimized multipole lenses* in place of the two-wire field lenses in this FODO lattice.

Figures 6(a) and 6(b) also show that most of the beam losses occur in the first 5 m and by 30 m the losses are essentially complete. This suggests that extending the beam transport line to much longer distances will not further reduce beam survival.

To find the most appropriate values of the lens decapole strength, for other molecules, we also studied beam survival for the two limiting cases of strong electric field (linear Stark effect) and weak electric field (quadratic Stark effect). A KV beam size of $a_{max}=2.5$ mm was used and the results, along with the results for methyl fluoride, are shown in Fig. 7.

For the strong field limit, as well as for the methyl fluoride example, we obtain the highest transmission for $a_5=0$. In the weak electric field limit the optimum value of a_5 is shifted to $a_5 \approx -0.2$, this nonlinearity in $\partial E/\partial x$ compensating the nonlinearity in $\partial W/\partial E$. Thus, an a_5 near zero would be a good choice for CsF molecules in low-lying rotational states, and an a_5 near -0.2 would be a good choice for ground-state atoms.

E. Velocity dependence of the beam transmission

So far we have considered only a monoenergetic beam. To look at the tolerance of the different lenses to energy deviations, we calculated the transmission for initially identical KV distributions but with different energies (560 m/s being the matched velocity).

The results are shown in Fig. 8, for KV beam size of $a_{max}=1.5$ mm, for both the two-wire field lens and for the optimized multipole lens. Both do quite well. At energies from 0.65 to 1.2 times the nominal energy of 640 K (velocity 560 m/s), transmission in the FODO lattice, of two-wire field lenses, is 50% or more of its maximum value. The FODO lattice of optimized multipole lenses does even better, as we would expect, since it has lossless transmission up to a KV size of $a_{max}=2.5$. One should note that Fig. 8 does not represent the energy acceptance of a complete transport line, which will be limited by the source and matching optics.

F. Beam matching and point focusing

We complete the model transport line by adding matching optics upstream and downstream of the FODO lattice. This matches the source to the lattice and the lattice to the final beam focus. The matching, in both cases, is achieved using a double- and a triplet-lens configuration as shown in Fig. 2. As the matching lenses require stronger focusing, producing more nonlinearities, we raise the lens scaling length in the matching lenses to $r_0=12$ mm. And since most of the beam losses occur early in the FODO lattice, we shorten the lattice to 9.5 m to reduce the computing time necessary for the simulation. The beam envelope, in x and y, and the placement of the lenses, is shown in Fig. 9, for an initial beam which is close to the linear focusing limit in the lenses.

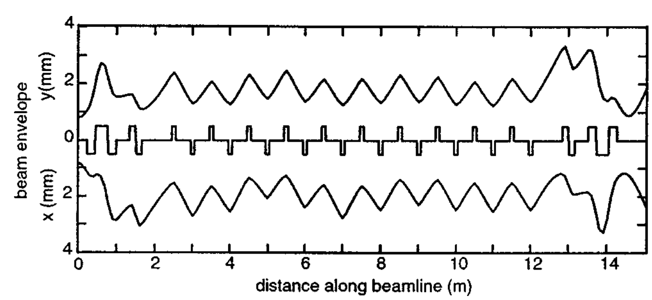

FIG. 9. Lens placement of a complete transport line with matching lenses and a 9.5 m FODO lattice (center line), and the calculated rms beam envelope, in x and y, for 560 m/s beam of methyl fluoride in the $J=0$ state. We model the beam from a skimmed jet source and focus it to a 2-mm-diam spot. A schematic of the beam transport line is shown in Fig. 2. With a central field of 3.2 MV/m, scaling length of $r_0=6$ mm for the FODO lattice lenses, and 12 mm for the matching lenses, the beam transport line has an acceptance of 2.5 mm mrad in both transverse planes. The longitudinal acceptance is about 84% for a $\pm 10\%$ rms energy spread.

For our example, of a 560 m/s beam of methyl fluoride in the $J=0$ state, we assume that the jet source has a very small orifice and a skimmer, of 1.5 mm diameter, is placed 25 cm upstream of the first lens. An angular spread of ± 3.3 mrad is fixed by collimators (see Fig. 2). This gives an initial beam emittance of 2.5 mm mrad in both transverse planes, and a maximum beam size of 2.1 mm in the FODO lattice. In addition, the initial beam is taken to have a Gaussian energy spread of $\pm 10\%$ (rms). The calculated beam transport, through this beamline, is 84% of the entering beam, the losses being due to the energy spread. Thus, we can transmit and focus most of the velocity distribution from the jet source. (If needed, the beam can be focused, at the end, to an even smaller size. However, in this case, we have to increase the size of the beam in the doublet/triplet lenses, where the nonlinear forces will produce emittance growth and beam halo. If we are not limited by the electric field strength, we can correct this by using lenses with a larger scaling length.)

G. Transmitted intensity

If the characteristics of the initial molecular beam are known, the transverse and longitudinal acceptances of the full beam transport line may be used to calculate the beam intensity at the final focus. As an example, consider the beamline in Sec. IV F, which has a skimmer radius of 0.75 mm and an angular acceptance of ± 3.3 mrad. From the point of view of an observer at the source, the entire beam transport line intercepts the same solid angle as would a 2-mm-diam collimator, located 0.3 m from the skimmer, with no lenses. The intensity of an unfocused beam at this location can (often) be calculated or measured. From this, and a knowledge of the rotational state population fraction, and the velocity spread, we can estimate the intensity at the final focus of the beamline.

For the methyl fluoride example, we assume a (seeded) jet-source beam temperature of 3.5 K. (This is based upon the equations in Ref. 18 for a 0.0035-cm-diam source orifice, a source pressure of 1.9×10^5 Pa (1400 Torr) of Ar at a reservoir temperature of 300 K, and a methyl fluoride seed of 5%. The source could be either pulsed or continuous.) The 3.5 K results in a $J=0$ population of about 30%, based upon a Maxwell–Boltzmann distribution, and a kinetic energy spread of 11.4% which implies a longitudinal acceptance of about 60%.

Thus an intensity, equivalent to 18% of an unfocused methyl fluoride beam passing through a 2-mm-diam collimator 0.3 m from the skimmer, would reach the final focus some 14.5 m from the source. And, since the beam transport line acceptances demonstrate transmission without loss, the same intensity should also reach a final focus much further from the source.

Finally, we note that much higher performance beam transport lines can be designed. If one uses stronger electric fields, shorter FODO cells, fill more of the beamline with focusing elements, and increases the size of the final focus, *most of the solid angle from the skimmer can be accepted.* Similar measures would allow one to efficiently transport and focus faster beams of molecules, such as those seeded in a helium jet source.

V. APPLICATIONS

Improving alternating gradient transport and focusing will make it easier to use molecules in strong-field seeking states for experiments, for beam transport, or to focus molecules for easier detection. In beam resonance experiments, molecules prepared in a strong-field seeking state can be detected, after a transition to a weak-field seeking state, as a flop-in resonance.

The optimized multipole lenses can greatly reduce the problem of Majorana transitions.[19,20] These are transitions that arise because different m_J levels belonging to the same J are degenerate in zero field. In very weak electric fields, a time-varying component caused, for example, by the motion of the molecule through the lens, can induce a transition to a different m_J state with a very different Stark effect. This leads to beam loss, or loss of signal and a large background in sensitive resonance experiments.

The optimized multipole lenses reduce this problem by allowing one to have all normal or all skew F and D lenses with their central electric fields in the same direction. This is done by changing the sign of a_3 the sextupole strength, while leaving the dipole strength (a_1) unchanged. Field direction changes in going between F lenses and D lenses are eliminated. If a weak dipole (bias) field is added to the region between the lenses, the molecules may never be in a rapidly changing weak electric field.

The problem of Majorana transitions will be greatest for molecules in weak-field seeking states focused by pure quadrupole and/or sextupole lenses. These lenses have a vanishing field at the center and rapid changes in the field direction at their entrances and exits.[7] The problem will be diminished if the molecules are focused in alternating gradient fields using optimized multipole lenses with their central electric fields in the same direction and with alternative positive and negative values of a_3. These lenses have a nonvanishing field everywhere and can be optimized for a quadratic Stark effect by choosing $a_5=-0.2$. Again a small dipole bias field can be used between lenses.

The problem of Majorana transitions can be eliminated by choosing the $J=0$ state, which is nondegenerate, always strong-field seeking, has the largest Stark effect of any rotational level, and is highly populated in a cold jet source beam.

The $J=0$ and other strong-field seeking states have unique and useful properties that can be exploited in experiments. Within a rotational level, J, the $|m_J|=J$ states are strong-field seeking. States that are strong-field seeking in weak fields remain strong-field seeking in stronger fields (but weak-field seeking states will become strong-field seeking in the limit of strong fields). Thus, for strong-field seeking states, there is no restriction on the strength of the electric field that can be used to focus them. This is an advantage for molecules with small rotational constants and large dipole moments, where the weak-field-seeking states in low rotational levels become strong-field seeking in modest electric fields. CsF (Fig. 1) and other heavy alkali halides are examples.

Long distance beam transport, which can exceed 100 m or more, has a number of applications. Since monatomic carrier gasses, clusters, and many contaminants will not focus through the beam transport line, it can be used to clean up a beam. For hazardous and radioactive molecules, a long beamline allows one to separate the source material and reservoir from the experiment and allows one to use radioactive detection in a lower background environment.

The long transit time (54 ms for the 30 m beamline in our example) corrected, if necessary for the small longitudinal velocity changes in the focusing elements, can be used for time-of-flight measurements with pulsed sources or a beam chopper. The different velocities will focus at slightly different longitudinal positions, which may be exploited for position-sensitive detection. Alternatively, by using a pulsed beam and ramping the electric field in the (final focus) lenses, all molecules may be brought to a focus, at different times, but at the same position.

The long flight path may be useful for collinear laser excitation of weak transitions. If the collinear laser excitation is combined with time-of-flight measurement, the Doppler spread from the velocity distribution may yield information about the absorption profile. Long transit time also allows for the decay of some long-lived states. Molecular beams may be run in both directions to form a very long colliding beam apparatus. In this case, the reservoir temperatures of the beam sources may be adjusted to equalize the focusing strengths of different molecules.

ACKNOWLEDGMENTS

The authors thank Jason Maddi for performing the Stark effect calculation used in Fig. 1 and, along with Daniel Schwan, for early assistance with this work. The authors thank Swapan Chattopadhyay for helping to get the work started. This work was supported by the Director, Office of Sciences, U. S. Department of Energy, and, in part, by the Office of Basic Energy Sciences, U. S. Department of Energy, both under Contract No. DE-AC03-76SF00098.

[1] D. Auerbach, E. Bromberg, and L. Wharton, J. Chem. Phys. **45**, 2160 (1966).
[2] D. Kakati and D. Lainé, Phys. Lett. **24A**, 676 (1967).
[3] D. Kakati and D. Lainé, Phys. Lett. **28A**, 786 (1969).
[4] G. Gunther and K. Schügerl, Z. Phys. Chem. (Munich) **NF80**, 155 (1972).
[5] A. Lübbert, F. Günther, and K. Schügerl, Chem. Phys. Lett. **35**, 210 (1975).
[6] A. Lubbert, G. Rotzoll, and G. Gunther, J. Chem. Phys. **69**, 5174 (1978).
[7] J. Reuss, in *Atomic and Molecular Beam Methods*, edited by G. Scoles (Oxford, New York, 1988), p. 276.
[8] H.-R. Noh, K. Shimizu, and F. Shimizu, Phys. Rev. A **61**, 041601 (2000).
[9] V. Cho and R. Bernstein, J. Phys. Chem. **95**, 8129 (1991).
[10] K. von Meyenn, Z. Phys. A **231**, 154 (1970).
[11] C. H. Townes and A. Schawlow, *Microwave Spectroscopy* (McGraw–Hill, New York, 1955).
[12] D. Schwan and J. Maddi (private communication).
[13] T. Miller, in *CRC Handbook of Chemistry and Physics*, 79th ed., edited by D. Lide (CRC, Boca Raton, 1999), Chap. 10, p. 160.
[14] T. Miller and B. Bederson, in *Advances in Atomic and Molecular Physics*, edited by D. Bates and B. Bederson (Academic, New York, 1977), Vol. 13, p. 1.
[15] J. A. Maddi, T. Dinneen, and H. Gould, Phys. Rev. A **60**, 3882 (1999).
[16] H. Bethlem, G. Berden, and G. Meijer, Phys. Rev. Lett. **83**, 1558 (1999).
[17] M. Kapchinsky and V. V. Vladimirsky, in *Proceedings of the International Conference on High Energy Accelerators and Instrumentation* (CERN, Geneva, 1959), p. 274.
[18] D. Miller, in Ref. 7, p. 14.
[19] E. Majorana, Nuovo Cimento **9**, 43 (1932).
[20] N. F. Ramsey, *Molecular Beams* (Oxford, London, 1956).